

# On the area of feasible solutions and its reduction by the complementarity theorem

Mathias Sawall<sup>a</sup>, Klaus Neymeyr<sup>a,b</sup>

<sup>a</sup>Universität Rostock, Institut für Mathematik, Ulmenstrasse 69, 18057 Rostock, Germany.

<sup>b</sup>Leibniz-Institut für Katalyse, Albert-Einstein-Strasse 29a, 18059 Rostock, Germany.

---

## Abstract

Multivariate curve resolution techniques in chemometrics allow to uncover the pure component information of mixed spectroscopic data. However, the so-called rotational ambiguity is a difficult hurdle in solving this factorization problem. The aim of this paper is to combine two powerful methodological approaches in order to solve the factorization problem successfully. The first approach is the simultaneous representation of all feasible nonnegative solutions in the area of feasible solutions (AFS) and the second approach is the complementarity theorem. This theorem allows to formulate serious restrictions on the factors under partial knowledge of certain pure component spectra or pure component concentration profiles.

In this paper the mathematical background of the AFS and of the complementarity theorem is introduced, their mathematical connection is analyzed and the results are applied to spectroscopic data. We consider a three-component reaction subsystem of the Rhodium-catalyzed hydroformylation process and a four-component model problem.

*Key words:* spectral recovery, multivariate curve resolution, nonnegative matrix factorization, area of feasible solutions, complementarity theorem.

---

## 1. Introduction

Multivariate curve resolution (MCR) methods in chemometrics are important and successful tools to extract information on the pure components from spectroscopic data of multi-component chemical reaction systems. However, MCR methods suffer from the so-called rotational ambiguity. This means that the factorization problem for the spectral data matrix often has wide ranges of nonnegative solutions. These solutions are called feasible factors. From these solutions the “true” nonnegative concentration profiles of the pure components and their associated spectra are to be selected. For two-component systems the observation of such continua of possible solutions has been made by Lawton and Sylvestre [1]. They also gave a representation of these continua of solutions by plotting the associated expansion coefficients in the plane. Such a representation of range of feasible solutions by sets of expansion coefficients is called an area of feasible solutions (AFS). For three-component systems Borgen and Kowalski [2] have devised a technique for representing the AFS also in the two-dimensional plane. For details on the construction of the AFS see [3, 4, 5, 6]. The numerical

computation of the AFS is very intensive in terms of computing time. For three-component systems efficient numerical processes have been presented in [7, 8, 9]. For four-component systems Golshan, Maeder and Abdollahi [10] recently presented a technique to compute the AFS.

### 1.1. Using supplemental information

Once having computed the AFS for a given spectral data matrix, one is interested in selecting one solution from the AFS which fits best the chemical system under consideration. Any further information on the reaction system can help to decrease the ambiguity and so to reduce the AFS. Various chemometric techniques have been developed to this end. Examples are the window factor analysis [11], the evolving factor analysis [12, 13], the application of unimodality conditions [14] or the use of kinetic models [15, 16, 17, 18] and last but not least the uniqueness theorems by Manne [19]. Another approach for feeding-in partial knowledge of the factors in order to reduce the rotational ambiguity is the *complementarity and coupling theory* which have been introduced in [20].

...

April 29, 2014

## 1.2. Aim and organization of this paper

The aim of this paper is to combine the complementarity theorem from [20] with the AFS for systems with an arbitrary number of components; practical applications are shown for three- and four-component chemical reaction systems. It is shown how the knowledge of a single spectrum, i.e. a single point of the spectral AFS, can reduce the AFS for the concentration factor for the remaining components to a straight line in case of a three-component system and vice versa, cf. [21, 9]. We also consider four-component systems where a pre-given point in the spectral AFS results in a plane in the AFS for the concentration factors. Such additional information on a chemical reaction system is sometimes accessible as the spectra of the reactants or the spectrum of the main product might be available. In other cases there are techniques to determine the concentration profiles of certain species. In Section 4 we consider experimental data from the Rhodium-catalyzed hydroformylation from which a catalytic subsystem with three components is studied.

The paper is organized as follows: After a brief introduction to the spectral recovery problem and to the AFS, the mathematical background for the application of the complementarity theorem to the AFS is discussed in Section 3. Numerical results are presented for a three-component system which is a subsystem of the Rhodium-catalyzed hydroformylation. Further a four-component model problem is studied.

## 2. Area of feasible solutions

### 2.1. The factorization problem

The key equation for the following analysis is the low-rank-approximation of the spectral data matrix  $D \in \mathbb{R}^{k \times n}$

$$D \approx \underbrace{U\Sigma T^{-1}}_C \underbrace{TV^T}_A, \quad (1)$$

which can be computed from a singular value decomposition [22] of  $D$ . Therein  $U$  is a  $k \times s$  matrix containing the first  $s$  left singular vectors of  $D$ , the  $n \times s$  matrix  $V$  contains the first  $s$  right singular vectors of  $D$  and  $\Sigma$  is the  $s \times s$  diagonal matrix with the  $s$  largest singular values on its diagonal, see [23, 24] for details. The regular  $s \times s$  matrix  $T$  serves to represent the rotational ambiguity. The desired approximate factors  $C$  and  $A$  of  $D$  can be computed by right-multiplication of  $U\Sigma$  with  $T^{-1}$  and left multiplication of  $V^T$  by  $T$ . Spectral recovery amounts to the construction of a suitable  $T$  by using

soft constraints, kinetic models or any other additional information, see e.g. [15, 16, 14, 25, 26].

A systematic and fundamental approach to the factorization problem is to compute and to represent the full set of all nonnegative solutions simultaneously. This complete representation is just the AFS. For an explanation of the AFS see the seminal papers of Borgen and Kowalski [2] as well as Rajkó and István [3]. Newer contributions on the numerical computation of the AFS for two-, three- and four-component systems can be found in [5, 7, 8, 9, 10].

### 2.2. Singular vector expansions

The representation of the AFS for the spectral factor is based on the expansion of the spectra with respect to the basis of right singular vectors given by  $V$ . In a similar way the AFS for the concentration factor rests on an expansion of the concentration profiles with respect to the basis of left singular vectors given by  $U$ .

In (1) the rows (spectra) of  $A$  are represented as linear combinations of the right singular vectors, which are the columns of  $V$ . The  $i$ th row of  $A = TV^T$  reads

$$\begin{aligned} A(i, :) &= (t_{i1}, \dots, t_{is})V^T = t_{i1} \underbrace{\left(1, \frac{t_{i2}}{t_{i1}}, \dots, \frac{t_{is}}{t_{i1}}\right)}_{=:x} V^T \\ &= t_{i1} (1, x)V^T. \end{aligned} \quad (2)$$

Therein  $t_{i1} \neq 0$  has been used, a fact which is by no means obvious, but has been proved in Theorem 2.2 of [9]. Equation (2) shows that the  $i$ th spectrum  $A(i, :)$  aside from scaling is uniquely determined by the row vector  $x \in \mathbb{R}^{s-1}$  of expansion coefficients. The scaling constant  $t_{i1}$  in (2) can be written as

$$t_{i1} = (T)_{i1} = (AV)_{i1} = (AV(:, 1))_i. \quad (3)$$

The construction for the factor  $C$  is similar. The  $j$ th column of  $C = U\Sigma T^{-1}$  with  $(T^{-1})_{ij} = \bar{t}_{ij}$  reads

$$\begin{aligned} C(:, j) &= U\Sigma(\bar{t}_{1j}, \dots, \bar{t}_{sj})^T \\ &= \bar{t}_{1j} U\Sigma \underbrace{\left(1, \frac{\bar{t}_{2j}}{\bar{t}_{1j}}, \dots, \frac{\bar{t}_{sj}}{\bar{t}_{1j}}\right)}_{=:y}^T \\ &= \bar{t}_{1j} U\Sigma(1, y)^T. \end{aligned} \quad (4)$$

Once again,  $\bar{t}_{1j} \neq 0$  is guaranteed by Theorem 2.2 in [9]. It holds that

$$\bar{t}_{1j} = (T^{-1})_{1j} = (\Sigma^{-1}U^T C)_{1j} = \sigma_1^{-1} U(:, 1)^T C(:, j). \quad (5)$$

### 2.3. The AFS

As shown in Equation (2) any spectrum can be represented (aside from scaling) by its vector  $x$  of expansion coefficients with respect to the right singular vectors  $V(:, 2), \dots, V(:, s)$ . This is the basis for a low dimensional representation of the AFS. A further argument is needed for the representation of the AFS, namely that by a permutation matrix  $P$  and its inverse  $P^T$  can be inserted between  $C$  and  $A$  in (1) and that this allows to rearrange the row of  $A$  and columns of  $C$  arbitrarily, since  $CA = (CP^T)(PA) = (U\Sigma T^{-1}P^T)(PTV^T)$ . Therefore only the first row of  $T$  is to be considered in order to define the AFS for the spectral factor. The delineation of the area of feasible solutions (AFS) under nonnegativity constraints for an  $s$ -component system is as follows

$$\begin{aligned} \mathcal{M}_A = \{x \in \mathbb{R}^{s-1} : \text{exists invertible } T \in \mathbb{R}^{s \times s}, \\ T(1, :) = (1, x), U\Sigma T^{-1} \geq 0 \text{ and } TV^T \geq 0\}. \end{aligned} \quad (6)$$

For a two-component system ( $s = 2$ ) the AFS is a real interval, for a three-component system ( $s = 3$ ) it is a subset in the plane and for  $s = 4$  it is a subset of the  $\mathbb{R}^3$ . For  $s = 2$  the interval-AFS can easily be written down explicitly. For  $s = 3$  geometric approaches to the construction of the AFS can be found in [2, 3]. Numerical methods for the computation of the AFS for  $s = 2, 3, 4$  are described in [5, 7, 10, 8, 9].

In a similar manner the AFS  $\mathcal{M}_C$  for the concentration factor can be defined. According to (4) and with the same arguments used above, matrices  $Z$  are to be determined with the first row equal to  $(1, \dots, 1) \in \mathbb{R}^s$  and with  $Z(:, 1)^T = (1, y)$  for  $y \in \mathbb{R}^s$  so that  $U\Sigma Z$  and  $Z^{-1}V^T$  are nonnegative matrices.

In short form  $\mathcal{M}_A$  and  $\mathcal{M}_C$  are given by

$$\begin{aligned} \mathcal{M}_A &:= \{x \in \mathbb{R}^{s-1} : U\Sigma T^{-1} \geq 0 \text{ and } TV^T \geq 0\} \\ \mathcal{M}_C &:= \{y \in \mathbb{R}^{s-1} : U\Sigma Z \geq 0 \text{ and } Z^{-1}V^T \geq 0\} \end{aligned} \quad (7)$$

with invertible  $s \times s$  matrices  $T$  and  $Z$  so that

$$T(1, :) = (1, x), \quad Z(:, 1)^T = (1, y)$$

and every matrix element of the first column of  $T$  and the first row of  $Z$  equals 1. For general data  $D$  the matrices  $T$  and  $Z^{-1}$  do not coincide since the restrictions on  $T$  and  $Z$  cannot be fulfilled simultaneously.

### 2.4. Block representation

For this paper it is useful to represent  $C$  and  $A$  and some of their submatrices by their expansion coefficients  $x$  and  $y$  according to (2) and (4). We call this the *block representation of truncated expansion coefficients* with respect to the basis of singular vectors.

**Definition 2.1.** Let  $s_0$  be an integer with  $1 \leq s_0 \leq s$  and let for  $i = 1, \dots, s_0$  the row vector  $x^{(i)} \in \mathbb{R}^{s-1}$  be the truncated vector of expansion coefficients of  $A(i, :)$  with respect to the right singular vectors in the sense of (2). Considering  $s_0$  rows of  $A(1 : s_0, :)$  simultaneously yields

$$X = \begin{pmatrix} x^{(1)} \\ \vdots \\ x^{(s_0)} \end{pmatrix} \in \mathbb{R}^{s_0 \times (s-1)}$$

as the block representation of truncated expansion coefficients.

In the same way let  $y^{(j)}$  be the representative of  $C(:, j)$  in the sense of (4). Then

$$Y = \begin{pmatrix} y^{(1)} \\ \vdots \\ y^{(s_0)} \end{pmatrix} \in \mathbb{R}^{s_0 \times (s-1)}$$

is the block representation of  $C(:, 1 : s_0)$ .

**Remark 2.2.** If  $s_0 = s$ , then the block representations  $X, Y \in \mathbb{R}^{s \times (s-1)}$  define two simplices in the  $\mathbb{R}^{s-1}$  whose vertices are the row vectors of either  $X$  or  $Y$ .

Further, Equations (2) and (3) result in

$$A(i, :) = (AV(:, 1)_i (1, x^{(i)}))V^T.$$

This yields for  $s_0 = s$  and with the  $s$ -dimensional 1-vector  $e = (1, \dots, 1)^T \in \mathbb{R}^s$

$$A = M_1(e, X)V^T \text{ with } M_1 = \text{diag}(AV(:, 1)).$$

Similarly, Equations (4) and (5) result in

$$C(:, j) = (\sigma_1^{-1}U(:, 1)^T C(:, j)) U\Sigma(1, y^{(j)})^T$$

so that for  $s_0 = s$

$$C = U\Sigma \begin{pmatrix} e^T \\ Y^T \end{pmatrix} M_2 \text{ with } M_2 = \text{diag}(\sigma_1^{-1}U(:, 1)^T C).$$

## 3. The AFS and the complementarity theorem

As stated in Section 1.1 there are various techniques how to feed in partial knowledge of the factors in order to reduce the rotational ambiguity of an MCR method. Here we would like to show how the complementarity theorem from [20] can be applied for the purpose of a reduction of the AFS.

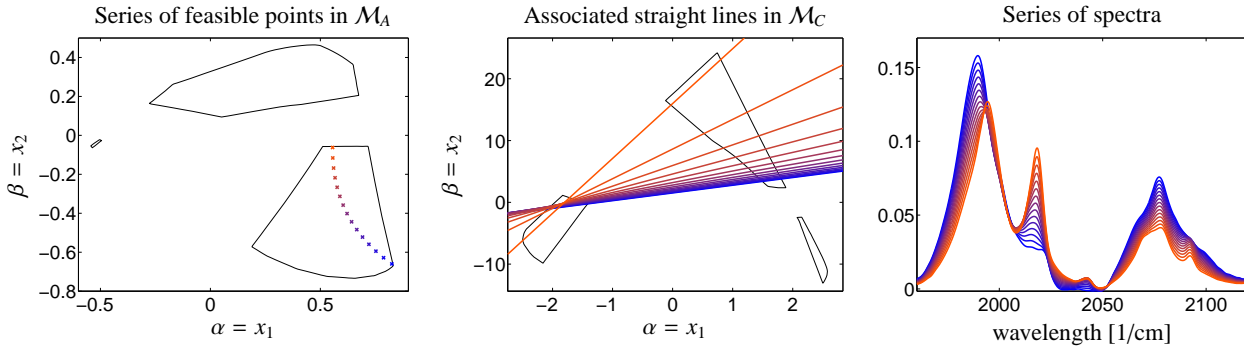


Figure 1: Application of Theorem 3.1 to an ( $s = 3$ )-component system for the Rhodium-catalyzed hydroformylation process, see Section 4.1 or [27] for details. Left: the spectral AFS is contoured by black lines and consists of three separated segments. A series of feasible spectra is shown by single points colored from blue to red. Right: the series of spectra which are associated with the series of points in  $\mathcal{M}_A$ . Center: Set of straight lines or one-dimensional affine subspaces in  $\mathcal{M}_C$  which are associated with the points in  $\mathcal{M}_A$  and which are shown in the same coloration. The axes of the AFS plots are  $x_1$  and  $x_2$ . For a three-component system these axes equal  $(\alpha, \beta)$  according to the standard notation.

### 3.1. Mutual reduction of $\mathcal{M}_C$ and $\mathcal{M}_A$ by the complementarity theorem

The complementarity theorem from [9] shows how pre-given spectra for certain pure components restrict the concentration profiles for the remaining components and vice versa. A comparable observation has been made in [21] for three-component systems.

For a reproduction of the complementarity theorem in concise form see Appendix 6.1. Next it is shown how such a pre-given spectrum, which is represented by a single point in the spectral AFS  $\mathcal{M}_A$  reduces the AFS  $\mathcal{M}_C$  for the complementary components.

**Theorem 3.1.** *Let a spectrum/row  $A(i_0, :)$  be given. According to (2) it holds  $A(i_0, :) = t_{i_0 1}(1, x)V^T$  and  $x$  specifies a point in the spectral AFS  $\mathcal{M}_A$ .*

*Then all concentration profiles  $C(:, j)$  with  $j \neq i_0$  are represented in the sense of (4) by points  $y$  which are elements of the  $s - 2$ -dimensional affine subspace*

$$C^{(i_0)} = \left\{ y \in \mathbb{R}^{s-1} : \sum_{\ell=1}^{s-1} x_\ell y_\ell = -1 \right\}. \quad (8)$$

*Thus all feasible concentration profiles  $C(:, j)$  with  $j \neq i_0$  have the form*

$$U\Sigma(1, y)^T \text{ with } y \in C^{(i_0)}.$$

*Proof.* For given  $A(i_0, :)$  Theorem 4.2 from [20], see also Appendix 6.1, can be applied (for the case that  $1 : s_0$  is substituted by  $i_0$ ). This theorem guarantees that the complementary concentration profiles  $C(:, j)$  for  $j \neq i_0$  are elements of the space

$$\{U\Sigma\tilde{y} : \text{for } \tilde{y} \in \mathbb{R}^s \text{ with } A(i_0, :)V\tilde{y} = 0\}. \quad (9)$$

Therein  $\tilde{y}$  is a column vector in the  $\mathbb{R}^s$ .

Insertion of  $A(i_0, :) = t_{i_0 1}(1, x)V^T$  into (9) shows that

$$t_{i_0 1}(1, x)V^T V\tilde{y} = t_{i_0 1}(1, x)\tilde{y} = 0 \quad (10)$$

is the decisive condition, which is now transformed in order to prove (8). First, Equation (4) allows to write the concentration profile  $C(:, j) = U\Sigma\tilde{y}$  in the form

$$U\Sigma\tilde{y} = \bar{t}_{1j}U\Sigma(1, y)^T$$

with the row vector  $y \in \mathbb{R}^{s-1}$ . Thus  $\tilde{y} = \bar{t}_{1j}(1, y)^T$ . Inserting this into (10) yields

$$t_{i_0 1}\bar{t}_{1j}(1, x)(1, y)^T = t_{i_0 1}\bar{t}_{1j} \left( 1 + \sum_{\ell=1}^{s-1} x_\ell y_\ell \right) = 0.$$

Since  $t_{i_0 1}\bar{t}_{1j} \neq 0$ , the second factor equals 0, i.e.  $\sum_{\ell=1}^{s-1} x_\ell y_\ell = -1$ , which proves (8).

Finally, the dimension of  $C^{(i_0)}$  equals  $s - 2$  because the vector  $y \in \mathbb{R}^{s-1}$  has to satisfy one linear constraint.  $\square$

The set  $C^{(i_0)}$  is an  $(s - 2)$ -dimensional affine subspace which is a hyperplane in  $\mathbb{R}^{s-1}$  and which intersects  $\mathcal{M}_C$ . Further, Theorem 3.1 also applies to the situation in which  $\mathcal{M}_A$  and  $\mathcal{M}_C$  have changed their places. This fact does not require a separate proof but is now stated explicitly.

**Corollary 3.2.** *Theorem 3.1 is applicable to the case in which  $A$  and  $C$  are swapped. Then a given representative  $y$  for a concentration profile  $C(:, i_0)$  results in the set*

$$\mathcal{A}^{(i_0)} = \left\{ x \in \mathbb{R}^{s-1} : x \cdot y^T = \sum_{\ell=1}^{s-1} x_\ell y_\ell = -1 \right\}$$

*of representatives for the complementary pure component spectra  $A(j, :)$  with  $j \neq i_0$ .*

Theorem 3.1 constitutes a relation between a certain point in either the spectral or concentrational AFS with an affine subspace in the concentrational or spectral AFS. For a two-component system a certain point  $x \in \mathcal{M}_A$  is directly related with another point  $y \in \mathcal{M}_C$ . For a three-component system a certain point  $x \in \mathcal{M}_A$  is connected with a straight line in  $\mathcal{M}_C$ , see also [21, 9]. This is demonstrated in Figure 1 where for the case  $s = 3$  a series of feasible points in  $\mathcal{M}_A$  is shown together with the set of associated one-dimensional affine subspaces (straight lines). Details on this problem are presented in Section 4.1. For an ( $s = 4$ )-component system a certain point  $x \in \mathcal{M}_A$  is related with a plane; this is demonstrated in Section 4.2 for a model problem.

If more than one spectrum or concentration profile of the pure components is known, then  $\mathcal{M}_A$  and  $\mathcal{M}_C$  can be further reduced. Then, in the best case, even a unique decomposition can be determined.

**Corollary 3.3.** *For given  $s_0$  rows  $A(i, \cdot)$ ,  $i = 1, \dots, s_0$ , let  $x^{(i)} \in \mathbb{R}^{s-1}$  be the representatives in the sense of (2). Let  $X \in \mathbb{R}^{s_0 \times (s-1)}$  be the block representation of these coefficients according to Definition 2.1.*

*Then the representatives  $y \in \mathcal{M}_C$  of the complementary columns  $C(:, j)$ ,  $j = s_0 + 1, \dots, s$ , are elements of the  $(s - s_0 - 1)$ -dimensional affine subspace*

$$\mathcal{C}^{(1:s_0)} = \left\{ y \in \mathbb{R}^{s-1} : Xy^T = (-1, \dots, -1)^T \right\}. \quad (11)$$

*Proof.* Let  $C(:, j)$  with  $j > s_0$  be a concentration profile and let  $y \in \mathcal{M}_C$  be its representative, see Equation (4). Theorem 3.1 imposes the conditions  $x^{(i)}y = -1$  for  $i = 1, \dots, s_0$ , which gives (11). The dimension of  $\mathcal{C}^{(1:s_0)}$  equals  $s - s_0 - 1$  since  $s_0$  linear equations are imposed on  $y \in \mathbb{R}^{s-1}$ .  $\square$

**Remark 3.4.** *The dimension  $s - s_0 - 1$  of  $\mathcal{C}^{(1:s_0)}$  is consistent with the dimension  $s - s_0$  in Equation (7) of Theorem 4.2 in [20]. The reason that the dimension of  $\mathcal{C}^{(1:s_0)}$  is reduced by 1 is that the block representation of the expansion coefficients in Definition 2.1 includes the fixed scaling of the first left singular vector. In other words,  $(1, y)$  is the vector of expansion coefficients under scaling assumptions and  $\omega(1, y)$ , for  $\omega \in \mathbb{R}$ , is the full subspace without any scaling.*

*Corollary 3.3 can also be formulated in a way in which  $C$  and  $A$  have changed their places.*

### 3.2. Simplices in $\mathcal{M}_C$ and $\mathcal{M}_A$ and their relations

In this section we assume that so much information on a factor is available that the second factor is completely determined by the complementarity theorem. A well known fact on MCR factorizations  $D = CA$  is that

one given factor determines the second factor. The second factor can be determined as follows: In the case of noise-free data  $D$  a linear system of equations is to be solved if  $CA$  has the full rank of  $D$ . In the case of noisy data or if a low-rank approximation of  $D$  is considered, then the second factor can be computed by solving least-squares problems. In any case the knowledge of a full factor completely determines the system.

A successful factorization means that in the AFS  $\mathcal{M}_A$  and the AFS  $\mathcal{M}_C$  each  $s$  points are specified. These points are the vertices of two simplices, one in  $\mathcal{M}_A$  and one in  $\mathcal{M}_C$ . For the factor  $A$  the simplex in  $\mathcal{M}_A$  has the vertices  $x^{(i)}$ ,  $i = 1, \dots, s$ , see (2). The block representation of these vertices is  $X \in \mathbb{R}^{s \times (s-1)}$  according to Remark 2.2. Analogously, the factor  $C$  defines a simplex in  $\mathcal{M}_C$  with the vertices  $y^{(j)}$  given by the rows of  $Y$ .

For a two-component system the simplex in  $\mathbb{R}$  is a line segment. For a three-component system the simplex in  $\mathbb{R}^2$  is a triangle and its edges are determined by the complementarity theorem 3.1. For four-components systems the simplex in  $\mathbb{R}^3$  is a tetrahedron and its side surfaces, the triangles, are determined by the complementarity theorem once again. All this is analyzed and demonstrated in the following. First the relation of the simplex defined by  $X$  to the simplex defined by  $Y$  is described in Theorem 3.5.

**Theorem 3.5.** *Let  $X \in \mathbb{R}^{s \times (s-1)}$  be the block representation of  $A$  as introduced in Definition 2.1. Then the vertices  $Y(j, \cdot)$ ,  $j = 1, \dots, s$ , can be computed by solving  $s$  linear systems of equations. For  $j = 1, \dots, s$  and  $Y(j, \cdot) = y^{(j)}$  the linear system of equations reads*

$$\begin{pmatrix} x^{(1)} \\ \vdots \\ x^{(j-1)} \\ x^{(j+1)} \\ \vdots \\ x^{(s)} \end{pmatrix} (y^{(j)})^T = \begin{pmatrix} -1 \\ \vdots \\ -1 \end{pmatrix}. \quad (12)$$

*The assertion also holds if  $X$  and  $Y$  are interchanged.*

*Proof.* Corollary 3.3 for  $s_0 = s - 1$  results in a 0-dimensional affine subspace  $\mathcal{C}^{(1:s-1)}$  which is just the single vertex  $Y(s, \cdot) = y^{(s)}$  and proves the case  $j = s$ . The argument can also be applied for the remaining indexes  $j$ .  $\square$

Theorem 3.5 and the simplices in  $\mathcal{M}_A$  and  $\mathcal{M}_C$  are illustrated by Figure 2 for a three-component system. Then the axes of the AFS plots are denoted by  $\alpha = x_1$

and  $\beta = x_2$  according to the standard notation. For details on the underlying factorization problem see Section 4.1.2.

**Remark 3.6.** *Theorem 3.5 in Equation (12) formulates a relation between the simplices in  $\mathcal{M}_C$  and  $\mathcal{M}_A$  which are defined by  $X$  and  $Y$ . This relation cannot immediately be translated to a factorization of  $D$  since the feasible factorizations*

$$D = \underbrace{U\Sigma T^{-1}}_C \underbrace{TV^T}_A = \underbrace{U\Sigma Z}_C \underbrace{Z^{-1}V^T}_{A'}$$

with  $T$  and  $Z$  defined in (7) include a specific scaling of the rows of  $A$  and columns of  $C$ . Thus in general  $C'A = U\Sigma ZTV^T \neq D$  holds. What is needed for a correct representation of the factorization are the two diagonal matrices  $M_1$  and  $M_2$  as introduced in Remark 2.2. With these matrices and with  $T = (e, X)$  and  $Z^T = (e, Y)$  for  $e = (1, \dots, 1)^T \in \mathbb{R}^s$  it holds that  $D = U\Sigma ZM_2M_1TV^T$ .

### 3.3. FAC-PACK implementation

In [9] a fast numerical procedure has been introduced for the numerical computation of the AFS  $\mathcal{M}_C$  and the AFS  $\mathcal{M}_A$  by the polygon inflation algorithm. A tutorial and the software, which is called *FAC-PACK* and which is written in C with a MatLab graphical user interface, are available from

<http://www.math.uni-rostock.de/facpack/>

The first revision *FAC-PACK* 1.0 serves to compute the spectral AFS  $\mathcal{M}_A$  and the concentrational AFS  $\mathcal{M}_C$ . The areas of feasible solutions which are shown in Figures 1 and 2 have been computed with *FAC-PACK*. In the first quarter of 2014 the revision 1.1 of *FAC-PACK* has been made publically available. This revision includes an algorithmic implementation of the complementarity theorem which allows to import known spectra or known concentration profiles, to mark their representatives in the AFS and to construct as well as to draw the complementary affine spaces. All the images shown in Figure 2 have been generated with the revision 1.1 of *FAC-PACK*.

### 3.4. A sensitivity measure with respect to noise

Theorem 3.1 and Equation (8) can be used to derive a relation on the sensitivity of the AFS with respect to noise.

**Lemma 3.7.** *Let  $x \in \mathcal{M}_A$  be given and let  $y \in \mathcal{M}_C$  be in the complementary space of concentration profiles*

as given by (8). If the perturbation of  $x$  due to noise is given by  $\delta_x$ , then the induced perturbation  $\delta_y$  of  $y$  is bounded as follows

$$\|\delta_y\| \geq \frac{|(\delta_x)y^T|}{\|x\|} \quad (13)$$

if the quadratic term  $(\delta_x)(\delta_y)^T$  is ignored. The inequality also holds with  $(x, \delta_x)$  and  $(y, \delta_y)$  having changed their positions.

*Proof.* Let a certain spectrum be given and let its representative be  $x \in \mathcal{M}_A$ . Theorem 3.1 shows that the representatives  $y$  of the complementary concentration profiles fulfill  $xy^T = -1$ . Let  $\delta_x \in \mathbb{R}^{s-1}$  be a perturbation (row) vector of  $x$  and  $\delta_y$  be the resulting perturbation for  $y$ . From

$$(x + \delta_x)(y + \delta_y)^T = -1$$

one gets after subtraction of  $xy^T = -1$

$$(\delta_x)y^T + x(\delta_y)^T = -(\delta_x)(\delta_y)^T = \mathcal{O}(\|\delta_x\| \|\delta_y\|)$$

where  $\mathcal{O}$  is the Landau symbol and where  $\|\cdot\|$  is the Euclidean vector norm. (The Landau or big O notation is used to describe the asymptotic behavior of a function; here it expresses that  $(\delta_x)(\delta_y)^T$  is a mixed quadratic term in the  $\delta$ -perturbations, which quadratically tends to 0, if  $\delta_x \rightarrow 0$  and  $\delta_y \rightarrow 0$ .)

Next the second order term of perturbations on the right-hand side is ignored. Application of the Cauchy-Schwarz inequality leads to

$$\|x\| \|\delta_y\| \geq |x(\delta_y)^T| = |(\delta_x)y^T|.$$

This proves that  $\|\delta_y\| \geq |(\delta_x)y^T|/\|x\|$ .  $\square$

Inequality (13) shows that the resulting perturbation  $\|\delta_y\|$  is bounded from below by  $|(\delta_x)y^T|/\|x\|$ . This lower bound is reciprocal to  $\|x\|$  which is the Euclidean distance of  $x$  to the origin. An interpretation of this result is as follows: For points  $x$  far away from the origin the influence of perturbations  $\delta_x$  on  $y$  decreases. However, any  $x$  close to the origin appears to be sensitive with respect to perturbations.

This perturbation argument is consistent with spectroscopic observations: For IR-spectra with narrow localized peaks next to non-absorbing frequency bands, the representatives  $x$  are often far away from the origin. Hence the sensitivity with respect to noisy data is relatively small. In contrast to this UV/Vis data often has wide absorbing frequency bands without non-absorbing bands. Then the representing vectors  $x$  of the true solutions are often close to the origin and the reliability of the results of Theorem 3.1 for noisy data decreases.

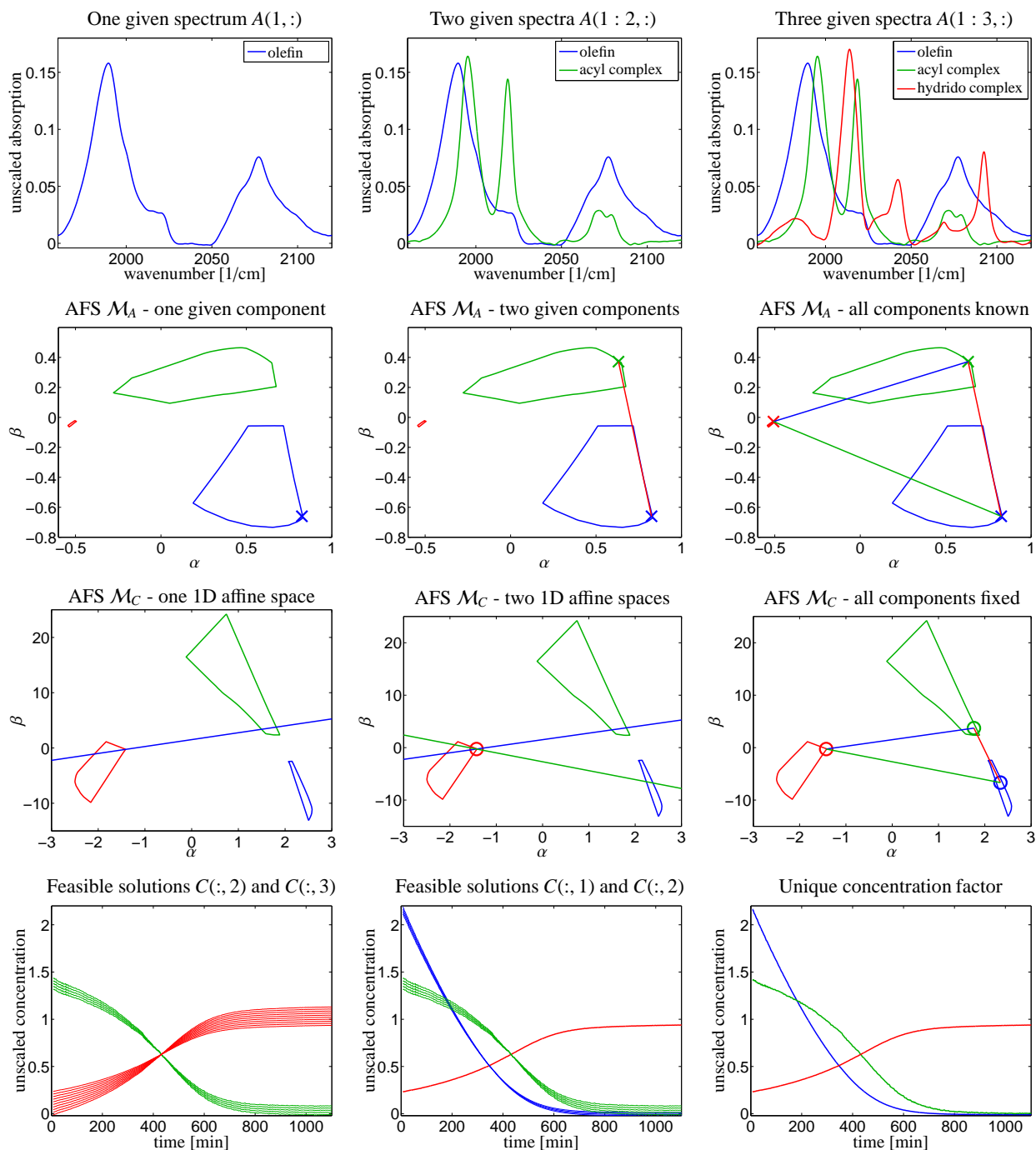


Figure 2: Application of Theorem 3.5 and Corollary 3.3 to spectral data from the Rhodium-catalyzed hydroformylation process, see Section 4.1. Left Column: One given spectrum fixes a point in  $\mathcal{M}_A$  and a straight line in  $\mathcal{M}_C$  for the complementary components. This results in one-dimensional continua of concentrations profiles. Center column: Two given spectra determine two points in  $\mathcal{M}_A$  and two straight lines in  $\mathcal{M}_C$ . Their intersection uniquely determines the concentration profile of the third component. Right column: Three given spectra completely determine the complete solution. The two simplices (triangles) in  $\mathcal{M}_A$  and  $\mathcal{M}_C$  according to Theorem 3.5 are also shown. First row: Given one, two and three spectra (rows of  $A$ ). Second row: AFS  $\mathcal{M}_A$  with one, two and three fixed points representing the given spectra. Third row: AFS  $\mathcal{M}_C$  with the affine subspaces according to Theorem 3.1 shown by one, two and three straight lines. The points of intersection of these lines uniquely determine concentration profiles. Fourth row: Series of concentration profiles which can be found in the intersection of the AFS with the affine subspaces (straight lines) according to Theorem 3.1. Known points in  $\mathcal{M}_A$  are marked by  $\times$  and are related with the straight lines in  $\mathcal{M}_C$ . Uniquely determined points in  $\mathcal{M}_C$  are marked by  $\circ$  and are associated with the edges of the triangle in  $\mathcal{M}_A$ . The same coloration is used for points in either  $\mathcal{M}_A$  or  $\mathcal{M}_C$  and their associated line segments in either  $\mathcal{M}_C$  or  $\mathcal{M}_A$ . A rescaling of the columns of  $C$  or rows of  $A$  is necessary for a correct reconstruction  $D = CA$ , cf. Remark 3.6.

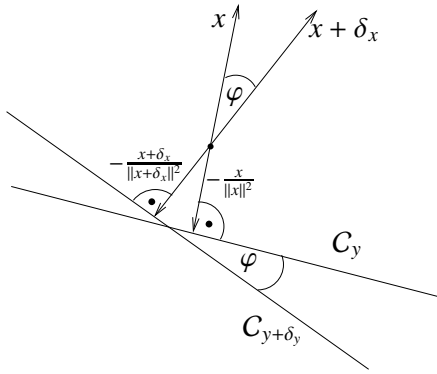


Figure 3: The geometric construction underlying Lemma 3.8.

The reciprocal relation between  $\|x\|$  and the perturbation  $\|\delta_y\|$  which is expressed by Equation (13) has some structural resemblance to the observation of Windig, Keenan et. al. [28] namely that in MCR techniques high contrast solutions in the  $C$ -space are related to low contrast solutions in the  $A$ -space and vice versa.

The next lemma shows that the acute angle which is enclosed by  $x$  and  $x + \delta_x$  in the  $A$ -space equals the acute angle which is enclosed by the associated one-dimensional affine spaces in the  $C$ -space and vice versa. This result can be interpreted as a bound on the potential perturbation  $\delta_y$  resulting from a given perturbation  $\delta_x$ . The application of this result to the AFS plots in the current paper requires that the  $\alpha$  and  $\beta$  axes are scaled to the same length units.

**Lemma 3.8.** *For ( $s = 3$ )-component system let  $x$  and  $x + \delta_x$  be given in  $\mathcal{M}_A$ . Further, let  $C_y$  and  $C_{y+\delta_y}$  be the associated one-dimensional affine linear subspaces as determined by Theorem 3.1. Then it holds that*

$$\angle(x, x + \delta_x) = \angle(C_y, C_{y+\delta_y}).$$

*The relation also holds if  $x$  and  $y$  interchange their positions.*

*Proof.* For a given  $x$  in  $\mathcal{M}_A$  any element  $y$  of the complementary space  $C_y$  satisfies  $(x, y) = x_1y_1 + x_2y_2 = -1$ . This relation can be rewritten in the Hesse normal form of a straight line

$$\left(-\frac{x}{\|x\|}, y\right) = +\frac{1}{\|x\|}.$$

This means that the  $C_y$  is a straight line which is orthogonal to  $-x/\|x\|$  and whose smallest distance to the origin is  $1/\|x\|$ .

Similarly the relation  $(x + \delta_x, y + \delta_y) = -1$  can be rewritten as

$$\left(-\frac{x + \delta_x}{\|x + \delta_x\|}, y + \delta_y\right) = +\frac{1}{\|x + \delta_x\|}$$

so that  $C_{y+\delta_y}$  is a straight line which is orthogonal to  $-(x + \delta_x)/\|x + \delta_x\|$  and whose smallest distance to the origin is  $1/\|x + \delta_x\|$ . The geometric setup is shown in Figure 3. Simple geometric arguments (on the sum of angles in a triangle) show that the acute angle  $\varphi$  which is enclosed by  $x$  and  $x + \delta_x$  equals the acute angle enclosed by  $C_y$  and  $C_{y+\delta_y}$ .  $\square$

### 3.5. Further AFS reduction effects

The complementarity theory is only one source for an AFS reduction from pre-given information. Next, three different sources for a reduction of the AFS are listed. We always assume that a single spectrum is known, i.e. a single point in the AFS  $\mathcal{M}_A$  is determined. (The same arguments apply if a single concentration profile or single point in the AFS  $\mathcal{M}_C$  is given.) Then, without claiming completeness, three different sources for restrictions on  $\mathcal{M}_A$  and  $\mathcal{M}_C$  are:

1. Restrictions on the AFS segments of the complementary components in  $\mathcal{M}_C$ . These restrictions are the topic of the present paper.
2. Restrictions on the concentration profile of the component for which the spectrum is given.
3. Restrictions on the AFS segments for the remaining components in  $\mathcal{M}_A$ .

The restrictions of the AFS due to the items 2 and 3 are presented in Figure 4 for the Rhodium-catalyzed hydroformylation process, see Section 4.1. Whilst item 1 enforces a restriction to a one-dimensional affine subspace, items 2 and 3 amount to a moderate decrease of the area of the AFS segments. Further details on item 3 are contained in [9]; the AFS restrictions related to item 2 will be explained in a forthcoming paper. In any case the predictions for  $\mathcal{M}_C$  by the complementarity theorem are much more restrictive compared to the other criteria.

### 3.6. Ambiguity reduction in MCR techniques

There are various further options for the reduction of the rotational ambiguity in multivariate curve resolution techniques. For instance hard-modeling by means of a kinetic model and the restrictions on the concentration profiles in  $C$  have been presented in [16]. Other important and well established techniques for the ambiguity reduction are the evolving factor analysis (EFA) and

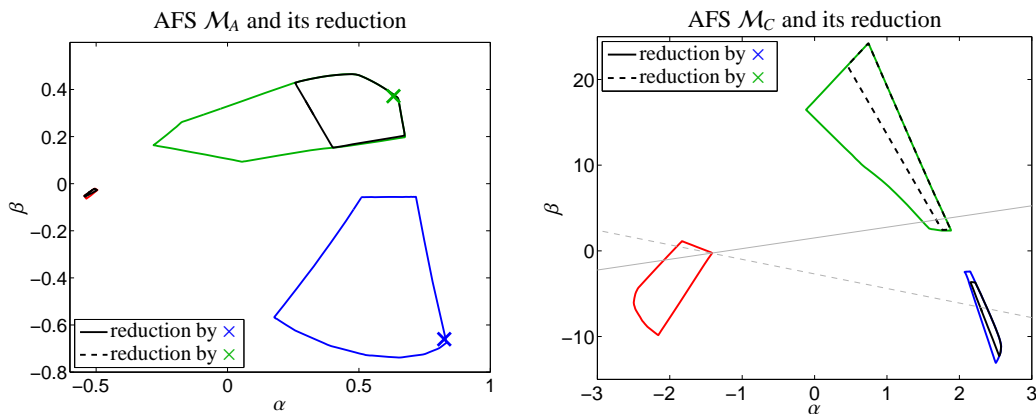


Figure 4: The AFS and its reduction for the spectral data from the hydroformylation process as considered in Figure 2. One or two points are fixed in  $\mathcal{M}_A$  and are marked by  $\times$  and  $\times$  in  $\mathcal{M}_A$ . The resulting reduced AFS segments are shown by a black solid line if only the point  $\times$  is given and by a broken line if only the point  $\times$  is given. In the left plot the broken line is contained in the small red segment. The restrictions by the complementarity theorem in  $\mathcal{M}_C$  are shown by two gray straight lines. These latter predictions are very restrictive since the intersection of the two straight lines determines one point in the red segment uniquely and the intersections with the green and the blue AFS segments are short line segments.

window factor analysis (WFA) [13, 12, 11] and techniques which exploit local rank information in order to extract single pure component spectra and single concentration profiles. For these techniques the Manne theorems are key tools [19].

It is worth noting that the complementarity theory is a hard constraint due to known spectra and concentration profiles which makes predictions on the remaining unknown parts of  $C$  and  $A$ . In this sense EFA and WFA are related to the complementarity theory. However, in this paper the focus is on the AFS and additional information, which may originate from a local rank analysis, is used in order to reduce the AFS for complementary components.

## 4. Numerical results

For the numerical experiments we consider a series of FT/IR spectra for a reactive subsystem of the Rhodium-catalyzed hydroformylation process with three components. We also treat a model problem with four components.

### 4.1. Rhodium-catalyzed hydroformylation

The first application is the Rhodium-catalyzed hydroformylation process. See [27, 8] for details on the reactive subsystem consisting of the olefin, the hydrido complex and the acyl complex. A total number of  $k = 1045$  spectra have been used within a wavenumber interval with  $n = 664$  channels. Hence  $D$  is a  $1045 \times 664$  matrix. The spectral AFS  $\mathcal{M}_A$  is shown in Figures 1 and 2. The

concentrational AFS  $\mathcal{M}_C$  is plotted in the third row of Figure 2. For this three-component system the standard notation  $\alpha = x_1$  and  $\beta = x_2$  is used.

#### 4.1.1. Series of feasible points

We start with a demonstration of the relation of points in  $\mathcal{M}_A$  and one-dimensional affine subspaces in  $\mathcal{M}_C$  as proved in Theorem 3.1. Figure 1 shows a series  $x^{(i)}$ ,  $i = 1, \dots, 15$ , of 15 feasible points in one segment of  $\mathcal{M}_A$ . If we assign to this segment of the AFS the component number 1, then the complementarity theorem says that the concentration profiles  $C(:, 2 : 3)$  are restricted to 1D affine subspaces in  $\mathcal{M}_C$ . For a fixed  $x = x^{(i)}$  the associated affine subspace is  $C^{(i)}$  and is given by (8). Figure 1 shows that the series of points in  $\mathcal{M}_A$  is associated with a series of 1D affine subspaces in  $\mathcal{M}_C$ . The dimension of each of these subspaces equals 1 since  $s = 3$  and only  $s_0 = 1$  spectrum is given. The associated series of spectra is also shown in Figure 1. A coloration from blue to red is used for the series of points in  $\mathcal{M}_A$ , for the associated 1D affine subspaces in  $\mathcal{M}_C$  and for the series of spectra.

#### 4.1.2. Successive reduction of the rotational ambiguity

Next Theorems 3.1 and 3.5 are applied in order to demonstrate the successive reduction of the rotational ambiguity for a three-component system. The effect of supplying additional information on the factors and the resulting predictions by the complementarity theorem is monitored in  $\mathcal{M}_A$  and  $\mathcal{M}_C$  simultaneously. Figure 2 shows all results. In the first row of this figure either

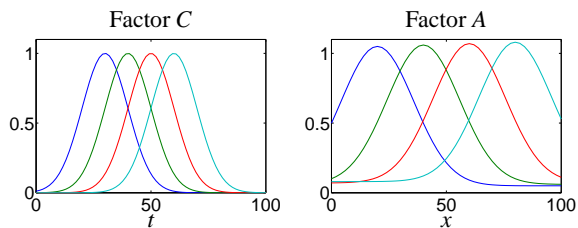


Figure 5: Four concentration profiles  $C \in \mathbb{R}^{70 \times 4}$  and the associated spectra  $A \in \mathbb{R}^{4 \times 51}$  of the simulated four-component model problem in Section 4.2.

one, two or three of the spectra are given. The second row shows the spectral AFS for the system with either one, two or three marked points which represent the given spectra. The third row shows the associated 1D affine subspaces in the concentrational AFS. If one spectrum is given, then the concentration profiles of the complementary components are restricted to a 1D affine space. If two spectra are given, then the concentration profile of one component is uniquely determined and for the remaining two components the concentration profiles are restricted to 1D spaces. If all three spectra are known, then all factors are uniquely determined. This situation is visualized in the right column of images in Figure 2. For this case two triangles (2D simplices) are shown in  $\mathcal{M}_A$  and  $\mathcal{M}_C$  according to Theorem 3.5. For all computations revision 1.1 of FAC-PACK has been used, see Section 3.3.

#### 4.2. A four-component model problem

The representation of an AFS by Equation (7) as well as the arguments of the complementarity theorem from Section 3 apply to any number of components  $s \geq 2$ . Next a ( $s = 4$ )-component model problem is considered. The simulated concentration profiles  $C \in \mathbb{R}^{70 \times 4}$  and the spectra  $A \in \mathbb{R}^{4 \times 51}$  are shown in Figure 5. The resulting spectral data matrix is  $D \in \mathbb{R}^{70 \times 51}$ .

##### 4.2.1. Reduction of the rotational ambiguity by the complementarity theorem

First the areas of feasible solutions  $\mathcal{M}_C$  and  $\mathcal{M}_A$  for  $D$  are computed. Every AFS consists of four separated segments which can be associated with the four components of the model problem. These segments are each approximated by a polyhedron whose surface is a 3D triangle mesh. These triangle meshes are shown in the first row of images in Figure 6. Then a first spectrum  $A(1, :)$  is fixed and the representative  $x \in \mathbb{R}^3$  is marked by a blue  $\times$  in  $\mathcal{M}_A$  together with a plane in  $\mathcal{M}_C$  to which  $C(:, 2 : 4)$  are restricted; see the second row of images in Figure 6. If a second spectrum  $A(2, :)$  is given whose

representative is marked by a green  $\times$  in  $\mathcal{M}_A$ , then a second plane can be added to  $\mathcal{M}_C$ . The intersection of these two planes in  $\mathcal{M}_C$  is a straight line (drawn by cyan color). This intersection combines the restriction on  $C(:, 2 : 4)$  and  $C(:, [1, 3 : 4])$  so that the concentration profiles  $C(:, 3 : 4)$  are described, see third row in Figure 6. Clearly,  $C(:, 1)$  is still represented by some point on the green plane and  $C(:, 2)$  by some point on the blue plane. If a third spectrum  $A(3, :)$  is fixed, then a third plane is added to  $\mathcal{M}_A$  and  $C(:, 4)$  is uniquely determined by the intersection of the three planes; see the last row in Figure 6. In the last image three lines are shown in cyan, yellow and magenta. These three lines are assigned to the three profiles  $C(:, i)$ ,  $i = 1, 2, 3$ , as pairs.

##### 4.2.2. The simplices in $\mathcal{M}_A$ and $\mathcal{M}_C$

Theorem 3.5 describes the relation of the two simplices  $\mathcal{M}_A$  and  $\mathcal{M}_C$  which each uniquely determine a feasible factorization. For our four-component system such a pair of feasible simplices is shown in Figure 7. These simplices are not independent of each other. As explained in Remark 3.6 the vertices of the simplices can be listed in the matrices  $T$  and  $Z$  and together with diagonal scaling matrices  $M_1$  and  $M_2$  a feasible non-negative factorization can be written down in the form  $D = (U\Sigma ZM_2)(M_1TV^T)$ .

## 5. Conclusion

The AFS is a powerful tool to study the rotational ambiguity and the band of feasible solutions of multi-variate curve resolution problems. However, the computation of all feasible solutions can only be a first step of a successful chemometric analysis of a spectroscopic data. Any further information on the reaction system should be used in order to decrease the rotational ambiguity. Such a decrease is equivalent with a reduction of the AFS. In the best case unique points in the AFS can be specified which uniquely determine one single factorization. A challenging point for the further application of AFS computations might be the analysis of multiway and multiset data [29]. Tauler, Maeder and de Juan [30] have devised a way how MCR-methods can be extended to the analysis of multiset data. Within this procedure the matricized form of the data can be an interface for the AFS techniques.

The complementarity theorem appears to be a valuable tool in order to support this reduction process. Any feed-in of pre-given or suspected spectra or concentration profiles can be used in order to define certain affine

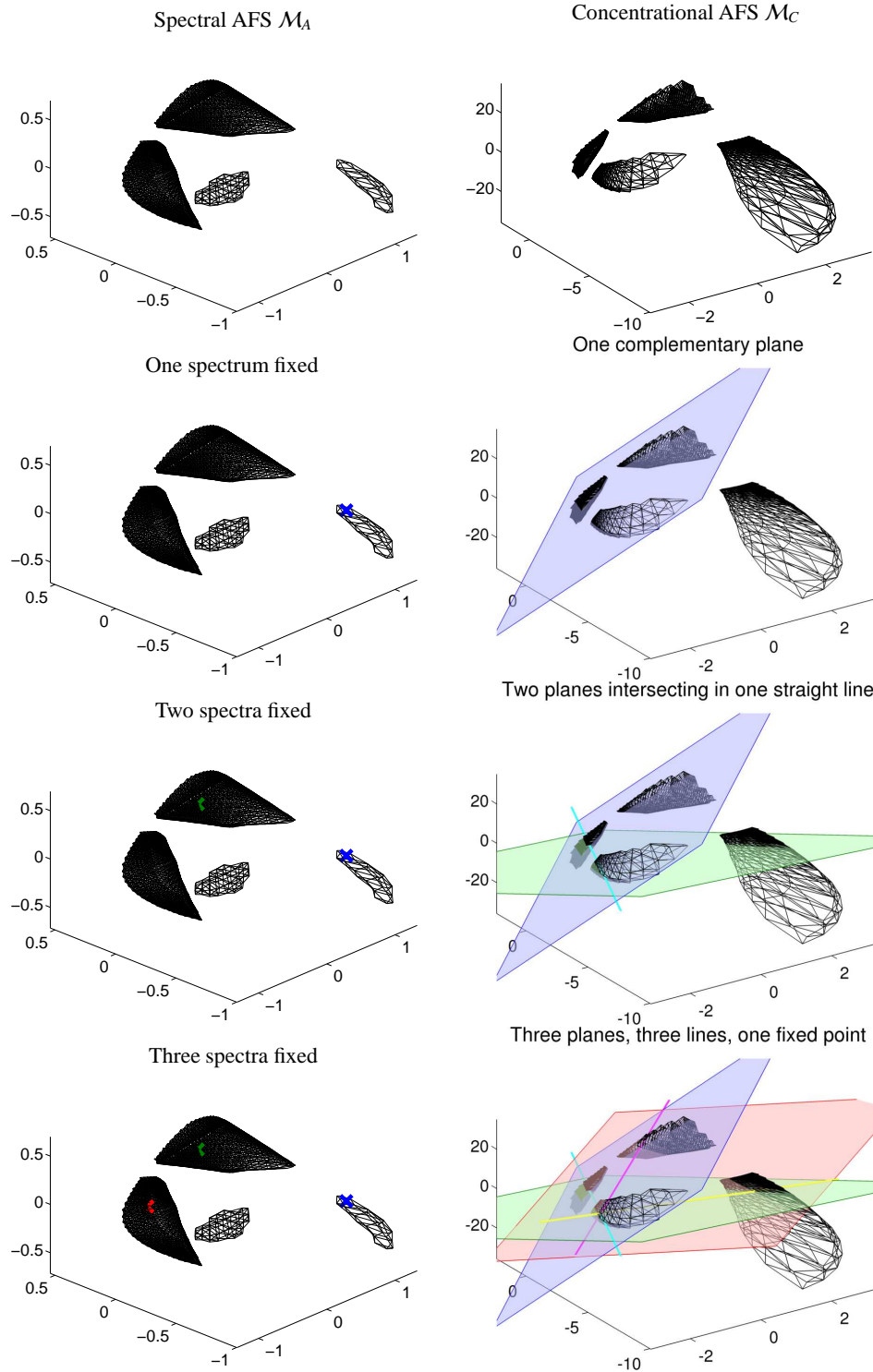


Figure 6: Successive reduction of the rotational ambiguity for a four-component system. First row: AFS  $\mathcal{M}_A$  and AFS  $\mathcal{M}_C$ . Second row: A certain spectrum  $A(1, \cdot)$  is fixed and Theorem 3.1 restricts  $C(:, 2 : 4)$  to the blue plane. Third row: Two spectra  $A(1, \cdot)$  and  $A(2, \cdot)$  in  $\mathcal{M}_A$ . The resulting two planes in  $\mathcal{M}_C$  intersect in a straight line (cyan) to which  $C(:, 3 : 4)$  are restricted. The coupled concentration profiles  $C(:, 1 : 2)$  in the sense of Theorem 4.6 in [20] are located on these planes. Fourth row: Three spectra are fixed, the coupled concentration profiles  $C(:, 1 : 3)$  are each on one line (cyan, yellow, magenta) and the complementary concentration  $C(:, 4)$  is uniquely given by the intersection of the three planes.

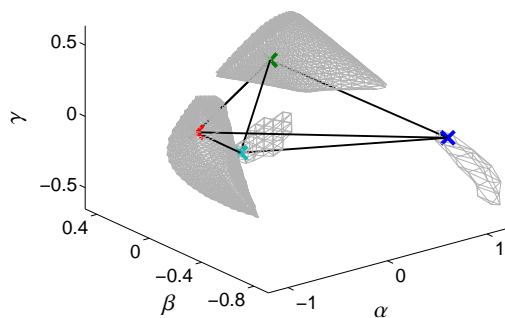
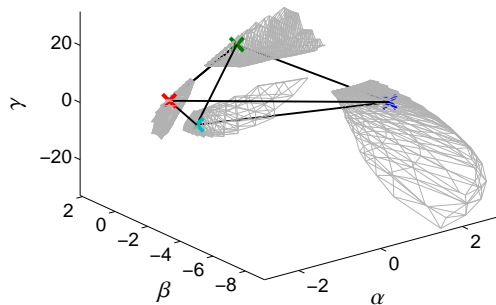
$\mathcal{M}_A$  and the tetrahedron of solutions $\mathcal{M}_C$  and the tetrahedron of solutions

Figure 7: Tetrahedra or 3-simplices for the pure factors shown in Figure 5. The two tetrahedra are related according to Equation (12) in Theorem 3.5. The colors of the vertices are consistent with those of the pure factors in Figure 5.

spaces to which the remaining factor are restricted. If multiple information from different sources is used, then multiple affine subspaces can be formulated. The intersection of these subspaces in the AFS can easily be interpreted as a further strong reduction of the rotational ambiguity. The mathematical theory behind the reduction of the AFS by the complementarity theorem has been implemented to the *FAC-PACK* software, see Section 3.3, and is available in its revision 1.1.

## Acknowledgment

The authors would like to thank H. Abdollahi and members of his group for the inspiring discussions on the topic of this paper at the 4th Iranian Biennial Chemometrics Seminar in Shiraz, Iran, in November 2013.

## 6. Appendix

### 6.1. Complementarity theorem

Next the complementarity theorem is reproduced. For its proof see [20].

**Theorem 6.1.** *Let  $D \in \mathbb{R}_+^{k \times n}$  be a matrix of rank  $s$ , which is assumed to be decomposable in the form  $D = CA$  with nonnegative factors  $C \in \mathbb{R}_+^{k \times s}$  and  $A \in \mathbb{R}_+^{s \times n}$ . Let  $U\Sigma V^T$  be a singular value decomposition of  $D$ . Further let the rows  $A(i, :)$  for  $i = 1, \dots, s_0$  be given.*

*Then all the complementary concentration profiles  $C(:, j)$  for  $j = s_0 + 1, \dots, s$  are contained in the  $(s - s_0)$ -dimensional linear subspace*

$$\{c \in \mathbb{R}^k : c \text{ has the form } c = U\Sigma y \text{ for a vector } y \in \mathbb{R}^s \text{ which satisfies } A(1 : s_0, :)Vy = 0\}. \quad (14)$$

The mathematical background of the complementarity theorem is the factorization

$$D = U\Sigma V^T = \underbrace{U\Sigma T^{-1}}_{=:C} \underbrace{TV^T}_{=:A}$$

where  $T$  is an invertible  $s \times s$  matrix. If some columns of  $C$  or some rows of  $A$  are known, then some linear constraints on  $T^{-1}$  or on  $T$  can be derived. Then the identity  $T^{-1}T = I$  allows to translate these constraints to the inverse factor, i.e., on  $T$  or on  $T^{-1}$ . In a final step these relations can be formulated as conditions on the factor  $A$  or on the factor  $C$ . The linear space (14) is the result of this analysis.

## References

- [1] W.H. Lawton and E.A. Sylvester. Self modelling curve resolution. *Technometrics*, 13:617–633, 1971.
- [2] O.S. Borgen and B.R. Kowalski. An extension of the multivariate component-resolution method to three components. *Analytica Chimica Acta*, 174:1–26, 1985.
- [3] R. Rajkó and K. István. Analytical solution for determining feasible regions of self-modeling curve resolution (SMCR) method based on computational geometry. *J. Chemometrics*, 19(8):448–463, 2005.
- [4] M. Vosough, C. Mason, R. Tauler, M. Jalali-Heravi, and M. Maeder. On rotational ambiguity in model-free analyses of multivariate data. *J. Chemometrics*, 20(6-7):302–310, 2006.
- [5] H. Abdollahi, M. Maeder, and R. Tauler. Calculation and Meaning of Feasible Band Boundaries in Multivariate Curve Resolution of a Two-Component System. *Analytical Chemistry*, 81(6):2115–2122, 2009.
- [6] H. Abdollahi and R. Tauler. Uniqueness and rotation ambiguities in Multivariate Curve Resolution methods. *Chemometrics and Intelligent Laboratory Systems*, 108(2):100–111, 2011.
- [7] A. Golshan, H. Abdollahi, and M. Maeder. Resolution of Rotational Ambiguity for Three-Component Systems. *Analytical Chemistry*, 83(3):836–841, 2011.

- [8] M. Sawall, C. Kubis, D. Selent, A. Börner, and K. Neymeyr. A fast polygon inflation algorithm to compute the area of feasible solutions for three-component systems. I: Concepts and applications. *J. Chemometrics*, 27:106–116, 2013.
- [9] Mathias Sawall and Klaus Neymeyr. A fast polygon inflation algorithm to compute the area of feasible solutions for three-component systems. II: Theoretical foundation, inverse polygon inflation, and FAC-PACK implementation. Accepted for *J. Chemometrics*, DOI: 10.1002/cem.2612, 2014.
- [10] A. Golshan, M. Maeder, and H. Abdollahi. Determination and visualization of rotational ambiguity in four-component systems. *Analytica Chimica Acta*, 796(0):20–26, 2013.
- [11] E.R. Malinowski. Window factor analysis: Theoretical derivation and application to flow injection analysis data. *J. Chemometrics*, 6(1):29–40, 1992.
- [12] M. Maeder. Evolving factor analysis for the resolution of overlapping chromatographic peaks. *Analytical Chemistry*, 59(3):527–530, 1987.
- [13] M. Maeder and A. D. Zuberbuehler. The resolution of overlapping chromatographic peaks by evolving factor analysis. *Analytica Chimica Acta*, 181(0):287–291, 1986.
- [14] R. Tauler. Calculation of maximum and minimum band boundaries of feasible solutions for species profiles obtained by multivariate curve resolution. *J. Chemometrics*, 15(8):627–646, 2001.
- [15] H. Haario and V.M. Taavitsainen. Combining soft and hard modelling in chemical kinetics. *Chemometr. Intell. Lab.*, 44:77–98, 1998.
- [16] A. Juan, M. Maeder, M. Martínez, and R. Tauler. Combining hard and soft-modelling to solve kinetic problems. *Chemometr. Intell. Lab.*, 54:123–141, 2000.
- [17] A. Golshan, H. Abdollahi, and M. Maeder. The reduction of rotational ambiguity in soft-modeling by introducing hard models. *Analytica Chimica Acta*, 709(0):32–40, 2012.
- [18] M. Sawall, A. Börner, C. Kubis, D. Selent, R. Ludwig, and K. Neymeyr. Model-free multivariate curve resolution combined with model-based kinetics: algorithm and applications. *J. Chemometrics*, 26:538–548, 2012.
- [19] R. Manne. On the resolution problem in hyphenated chromatography. *Chemometrics and Intelligent Laboratory Systems*, 27(1):89–94, 1995.
- [20] M. Sawall, C. Fischer, D. Heller, and K. Neymeyr. Reduction of the rotational ambiguity of curve resolution techniques under partial knowledge of the factors. Complementarity and coupling theorems. *J. Chemometrics*, 26:526–537, 2012.
- [21] S. Beyramysoltan, R. Rajkó, and H. Abdollahi. Investigation of the equality constraint effect on the reduction of the rotational ambiguity in three-component system using a novel grid search method. *Analytica Chimica Acta*, 791(0):25–35, 2013.
- [22] G.H. Golub and C.F. Van Loan. *Matrix Computations*. Johns Hopkins Studies in the Mathematical Sciences. Johns Hopkins University Press, 2012.
- [23] M. Maeder and Y.M. Neuhold. *Practical data analysis in chemistry*. Elsevier, Amsterdam, 2007.
- [24] E. Malinowski. *Factor analysis in chemistry*. Wiley, New York, 2002.
- [25] J. Jaumot and R. Tauler. MCR-BANDS: A user friendly MATLAB program for the evaluation of rotation ambiguities in Multivariate Curve Resolution. *Chemometrics and Intelligent Laboratory Systems*, 103(2):96–107, 2010.
- [26] K. Neymeyr, M. Sawall, and D. Hess. Pure component spectral recovery and constrained matrix factorizations: Concepts and applications. *J. Chemometrics*, 24:67–74, 2010.
- [27] C. Kubis, D. Selent, M. Sawall, R. Ludwig, K. Neymeyr, W. Baumann, R. Franke, and A. Börner. Exploring between the extremes: Conversion dependent kinetics of phosphite-modified hydroformylation catalysis. *Chemistry - A European Journal*, 18(28):8780–8794, 2012.
- [28] W. Windig and M.R. Keenan. Angle-constrained alternating least squares. *Appl. Spectrosc.*, 65:349–357, 2011.
- [29] A. Smilde, R. Bro, and P. Geladi. *Multi-way Analysis. Applications in the Chemical Sciences*. Wiley, 2004.
- [30] R. Tauler, M. Maeder, and A. de Juan. Multiset data analysis: Extended multivariate curve resolution. In S.D. Brown, R. Tauler, and B. Walczak, editors, *Comprehensive Chemometrics, Chemical and biochemical data analysis*, volume 2, pages 473–505. Elsevier, 2009.